



Fin actuation, thrust vector control and landing leg mechanisms design for the RETALT VTVL launcher

Anett Krammer¹ · Luc Blecha¹ · Marc Lichtenberger¹

Received: 15 July 2021 / Revised: 15 November 2021 / Accepted: 31 December 2021 / Published online: 13 January 2022
© The Author(s) 2022, corrected publication 2022

Abstract

To foster the competitiveness of the European industry in the global launcher market, the need arose to build up the necessary know-how on state-of-the-art vertical take-off vertical landing (VTVL) concepts and corresponding technologies. In the EU Horizon 2020 project RETALT (RETro propulsion Assisted Landing Technologies), the VTVL approach applying retro propulsion is investigated for two-stage-to-orbit (TSTO) and single-stage-to-orbit (SSTO) reusable launch vehicles, these configurations are named RETALT1 and RETALT2. In the project framework investigation of both reference configurations is performed in several areas: aerodynamics, aerothermodynamics, flight dynamics and guidance, navigation, and control (GNC), as well as thermal protection and structures and mechanisms. Focusing on solutions for the RETALT 1 launch vehicle, Almatech contributes with the design of mechanisms to actuate the aerodynamic control surfaces, retain and deploy the landing legs and provide means to dissipate energy during touch-down. Demonstrators of these mechanism are also built during the project. In addition to the above activities, Almatech proposes thrust vectoring solutions. This paper presents an overview of these activities and results obtained so far.

Keywords Mechanisms · Aerodynamic control surfaces · Fin · Landing leg · Shock absorber · Deployment · Thrust vector control · Gimbal

Abbreviations

ACS	Aerodynamic control surface
CFD	Computational fluid dynamics
CFRP	Carbon fiber reinforced polymer
CoG	Center of gravity
CoP	Center of pressure
GNC	Guidance, navigation, and control
GTO	Geostationary transfer orbit
HDRM	Hold down and release mechanism
LEO	Low earth orbit
LOX/LH2	Liquid oxygen and hydrogen
RCS	Reaction control system
RETALT	RETro propulsion assisted landing technologies
RLV	Reusable launch vehicle
SSTO	Single-stage-to-orbit
TSTO	Two-stage-to-orbit

TVC	Thrust vector control
VTVL	Vertical take-off, vertical landing

1 Introduction

RETALT is a project funded by the European Union's Horizon 2020 research and innovation framework program. Its objective is to investigate technologies for reusable, vertical take-off, vertical landing (VTVL) launch vehicles applying retro propulsion. The investigated configurations are named: RETALT 1—two-stage-to-orbit (TSTO), and RETALT2—single-stage-to-orbit (SSTO).

Within the identified key technologies are aerodynamic control surfaces, landing legs and thrust vector control. Work Package 5 of the project addresses the design of these technologies. The involved structures and mechanisms are developed through close collaboration between MT Aerospace—responsible for structures, and Almatech—developing the mechanisms. The most promising solutions for aerodynamic control surfaces and landing leg systems are carried forward to large scale manufacture and demonstration. Additionally, Almatech performs a trade-off on thrust vector control (TVC) solutions

✉ Luc Blecha
Luc.Blecha@almatech.ch

¹ Almatech, EPFL Innovation Park, Bâtiment D,
1015 Lausanne, Switzerland

answering the RETALT requirements to define a concept which can be used on the different types of rocket engines.

This paper presents the development philosophy and high-level concept definition of the mechanisms for the RETALT1 configuration. The paper is organized in three main parts: presentation of the vehicle layout and relevant concept of operations, followed by the review of the key design drivers, then discussion of the current status of concept generation and mechanism design. While activities for the aerodynamic control surfaces and thrust vector control are nearly completed, landing leg detailed design activities have just started as of the submission of the present paper.

2 RETALT1 vehicle description and concept of operations

The design of the mechanisms is based on the first stage of RETALT1—a reference configuration for the study of the selected key technologies, as presented in [1], and specifically answer to the requirements of the descent phase of the mission.

RETALT1 is a TSTO heavy lift launcher that can carry 14 tons to geostationary transfer orbit, with a configuration similar to that of the SpaceX launch vehicle: Falcon 9, or the Blue Origin launch vehicle: New Glenn. The first stage is powered by nine engines—similar to the Vulcain 2 engines used on the Ariane launch vehicle—with liquid oxygen and hydrogen (LOX/LH₂) as oxidizer and fuel. Figure 1 shows the outline of the RETALT1 configuration.

The deceleration of the first stage during return flight is performed with the main engines, which can be supported by the aerodynamic control surfaces (see discussion in Sect. 4.1). Descent trajectories vary depending on the mission. For low earth orbit (LEO) missions, the first stage can perform a return to launch site, while for GTO missions down range landing on a sea platform can be performed. Figure 2 presents the corresponding principal flight phases.

Aerodynamic control surfaces are deployed before the first stage reenters the denser atmosphere. Then, a first braking maneuver is performed followed by the main engine cut-off and a ballistic phase. Finally, the first stage is decelerated further with the landing burn of the central engine until touch-down. Thrust vector control (TVC) is used for low-speed maneuvering and the landing legs deploy shortly before touch-down with mechanism to dissipate the landing energy.

3 Review of key mechanism design drivers

International competition and developments are ongoing aiming to reduce the cost of access to space. One of the key cost reduction drivers is the ability to reuse certain expensive

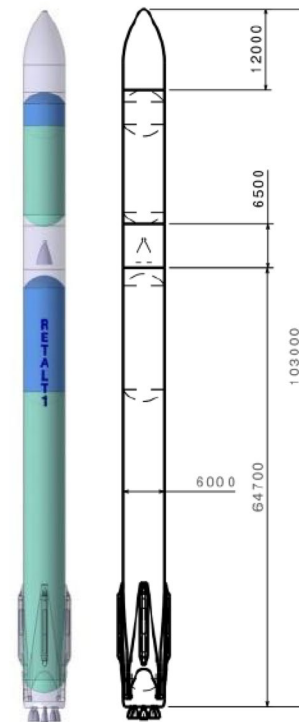


Fig. 1 RETALT 1 outline [1]

parts of the launch vehicle for several launches. The vehicle's reusability comes at a price of additional equipment and technologies that impact launcher direct and indirect costs, such as maintenance and mass increase. To achieve average cost reduction over multiple flights, these extra costs shall be much lower than the costs of new non-reusable parts necessary for the given number of flights. The low-cost requirement also implies low mass to be able to maximize payload fraction, and low maintenance to minimize downtime. Furthermore, the mechanisms involved shall be highly reliable, which is especially important as components of a reusable vehicle see longer service life than those of an expendable one, and they must answer the additional requirements of return and landing operations as well. The main design drivers are addressed below and discussed in relevance to each mechanism in Sect. 4.

3.1 Cost-effectiveness

Standardized components and processes are considered, the use of exotic materials and processes are to be minimized as much as possible to reduce cost. Simplicity, which can translate into modularity, facilitates quick and cost-effective development. Manufacturing and assembly reproducibility are important parameters for cost control.

As the mechanisms are to satisfy reusability requirements, reparability and component damage tolerance shall

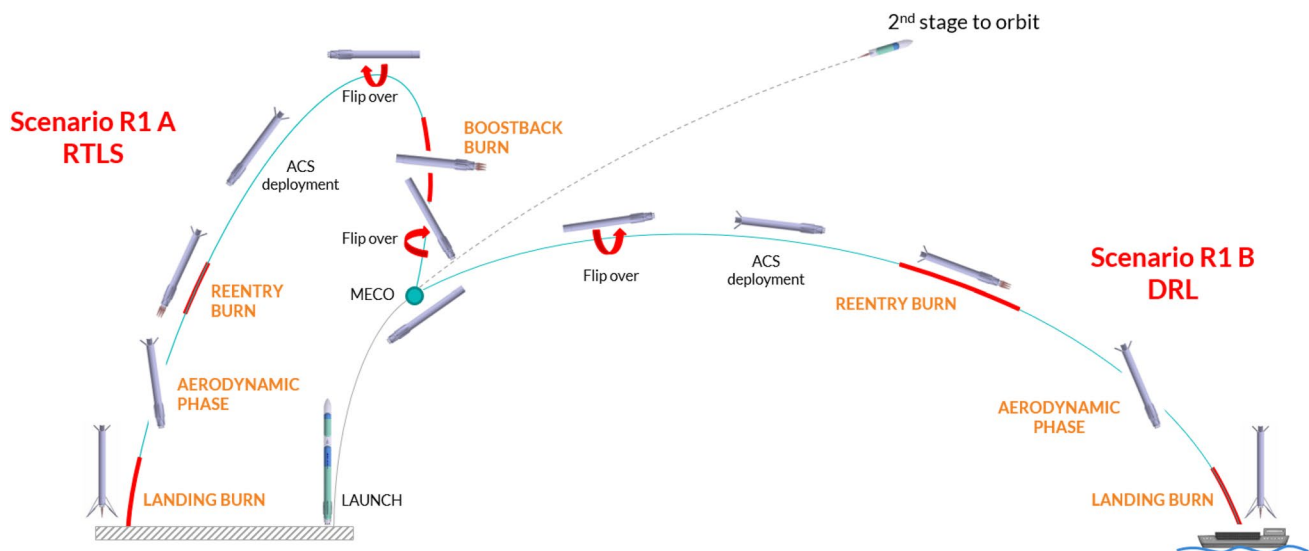


Fig. 2 RETALT 1 principal flight phases [2]

be taken into account when choosing components and thermal protection. In general, increasing life of components, mainly those with higher failure rates, is key to make the reusable concept cost-effective.

Due to the nature of the vehicle, considerations enabling rapid reuse are important during design and development to facilitate minimizing downtime: simplifying operations, related equipment as well as procedures for launch preparation, refurbishment, maintenance, and repair. Therefore, ease of refurbishment and/or replacement of components is paramount along with ease of access and installation, as well as disassembly—as an important aspect of operations and maintenance of the launch vehicle is transportability. Due to these reasons, a modular approach is preferred whenever possible.

Additionally, the design shall take into consideration: low mass, compactness, and impact on other systems such as electrical interface demands including power, and impact on structures.

3.2 Reliability

Reliability of a mechanism decreases with increasing complexity; therefore, the number of moveable parts shall be minimized wherever possible. Redundancy is to be considered for most critical components. Further reliability-associated considerations are: failure modes criticality, sensitivity to contamination, material environment exposure adequacy (thermal, radiation, ablation, etc.), representativity of on-ground testing, and reliability of performance predictions over life.

Complexity of the mechanism and assembly shall be minimized by reducing the number of parts, and assembly

and control steps. Whenever possible, commonality of components is favored, for instance the use of identical actuators, bearings, etc.

4 Mechanism concept generation and design

In addition to the general design drivers presented in Sect. 3, the mechanism design has to take into consideration impact on other vehicle systems such as structures, aerodynamics, guidance, navigation, and control (GNC), electrical power systems, etc. As the choice of solution has a system-level impact, the structures and mechanism concepts and requirements have evolved during the project. Specific design drivers and corresponding solutions were identified and are discussed hereafter.

4.1 Aerodynamic control surfaces

4.1.1 Control surface concept selection

The main functional requirements of the aerodynamic control surfaces are:

- The control surfaces shall deploy before the first breaking maneuver.
- The control surfaces shall provide pitch and yaw inputs to the launcher during the aerodynamic descent phase.

Three types of aerodynamic control surfaces are explored in the project for RETALT1: petals, grid fins and planar fins. The three concepts are shown on Fig. 3.

For RETALT1, the control surfaces are stowed for launch and during ascent, and are deployed following stage separation, in the descent phase of the first stage, but still at high altitude, at low aerodynamic pressure conditions to minimize aerodynamic loading at deployment. At this altitude, the hold-down mechanism is released and the control surfaces are driven to nominal position, then actuated at demand.

Petals are a novel solution proposed for the RETALT project, where the interstage is segmented, and segments deploy to provide drag augmentation aiding slowing down the vehicle. Operating the petals against the airflow generates high aerodynamic loads. While differential actuation of the surfaces allows the control of pitch and yaw, dynamically moving such large surfaces over high rotation angles (up to 45°) to effectively to trim the vehicle is challenging from a structures and mechanisms point of view.

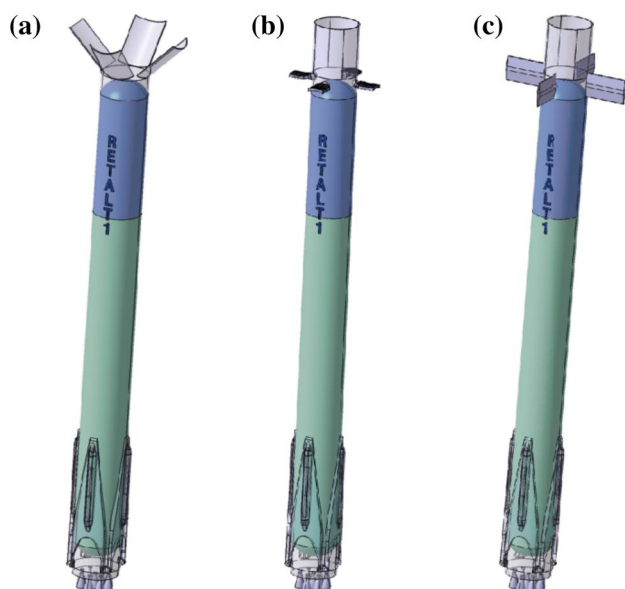


Fig. 3 RETALT1 aerodynamic Control Surface options: **a** petals, **b** grid fins, **c** planar fins [3]

Grid fins are lattice-structure control surfaces traditionally used on missiles and also implemented on the SpaceX Falcon 9 launchers. During operation, these fins are perpendicular to the airflow, thus their deployment from the stowed position to their nominal position can be implemented in a single step.

Planar fins are classical control surfaces used on guided missiles and can be seen on the New Shepard and New Glenn launchers of Blue Origin. For RETALT1, these surfaces would be stowed along the launch vehicle main axis and deploy in two steps to their nominal position: parallel to the airflow.

All three control surface types are investigated for GNC feasibility and aerodynamic performance. In addition, petals and planar fins are examined for feasibility from a structures and mechanisms point of view, with mechanism performance requirements generated from mission engineering studies. As petals are primarily drag augmentation devices and planar fins are control surfaces, the derived performance requirements are not equivalent between these configurations.

4.1.2 Petal and fin-mechanism overview

Petals and fins have different roles, and the involved mechanisms have to fulfill different functions. These roles and functions are summarized in Table 1.

The definition of axes for the planar fins are shown on Fig. 4.

4.1.3 Petal and fin hinge moments

Forces/torques seen by the mechanism actuators have the following main contributions:

- Aerodynamic forces,
- Forces due to control surface and component inertia,
- Friction forces (e.g., bearing friction),

Table 1 High level overview of ACS concepts

	Petals	Fins
Control surface role	Control/trim and aerodynamic breaking; Control of pitch and yaw with differential actuation of petals	Control/trim; Control of pitch, yaw (roll possible)
Structure	Integrated in interstage structure	Stowed against launcher body, not part of interstage structure
Mechanism functions	Disengage petal lock; Deployment and operation around hinge line	Disengage fin lock; Deployment: rotate 90° around axis1, Lock axis 1 so rotation around this axis is no longer possible, Bring to nominal position: rotate 90° around axis2; Operation: $\pm 20^\circ$ around axis2

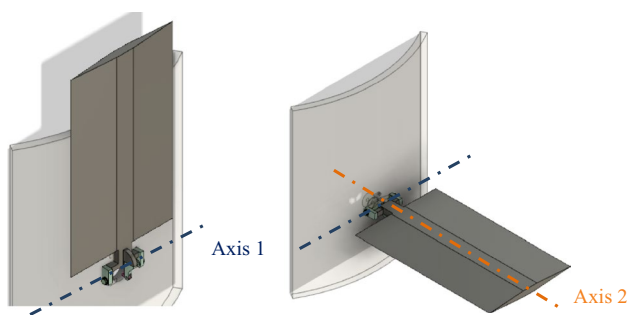


Fig. 4 Deployment of planar fins—axis definitions

- Forces due to flexible structures (e.g., harness).

Concept feasibility is evaluated for both petals and fins with simplified analysis by considering the two main contributions to the generated hinge moment: worst-case aerodynamic loading and loading due to control surface inertia.

Each petal is considered to be a 90° segment of the interstage, with a height of 3.8 m. A normal force of 355 kN acts at the center of pressure (CoP) location. Petals are to be deflected by 45° at a deflection rate of 15°/s. The hinge line is given by the petal definition: it is located at the interface between the first stage and the interstage.

The fin has a hexagonal profile, with a chord length of 3 m and span of 5 m. In the subsonic regime, the maximum normal force on the fin is 180 kN, while in the supersonic regime a maximum of 350 kN normal force acts on the fin. Hinge moments are derived with these maximum forces considered at maximum fin deflection, at 20°. The location of the CoP between the subsonic and supersonic regimes varies from a nominal location of 25% of the chord, to 40% of the chord. Therefore, an “ideal” hinge line location, illustrated on Fig. 5, is identified between these two locations, to minimize the required hinge moment. Hinge line location is

estimated taking into account the maximum normal forces on the fin and the corresponding worst-case center of pressure locations: i.e., minimum distance from the leading edge for the subsonic, and maximum distance for the supersonic range.

Induced moments, for both petals and fins (torque around axis 2), due to operation around the hinge line have been estimated and are summarized in Table 2 below.

The hinge moment required to move a single petal is a factor of seven greater than the hinge moment required to operate a single fin. For both petal and fin, aerodynamic loads drive the hinge moment. Ultimately, minimizing distance between center of pressure and hinge line location would minimize hinge moment, which could greatly relax actuation requirements.

4.1.4 Fin mechanism design: concept of operations

Due to the large hinge moment requirements of the petals, induced requirements on the structures involved, as well as GNC and other system considerations, deployable planar fins have been chosen as a baseline configuration for the aerodynamic control surface concept generation.

Fins deploy from the stowed configuration by a rotation of 90° around axis 1 (Fig. 4). To bring them into nominal position, they are turned by 90° around axis 2. Overview of the resulting fin deployment sequence is presented on Fig. 6.

Fins are operated around their nominal position by a rotation around axis 2 of ±20°. Mechanism operational rotation is presented on Fig. 7.

4.1.5 Fin mechanism design: design description

Several actuators and axis locking are used in the actuation chain to facilitate decoupling load paths for different phases of the actuation. Actuation requirements and loads involved

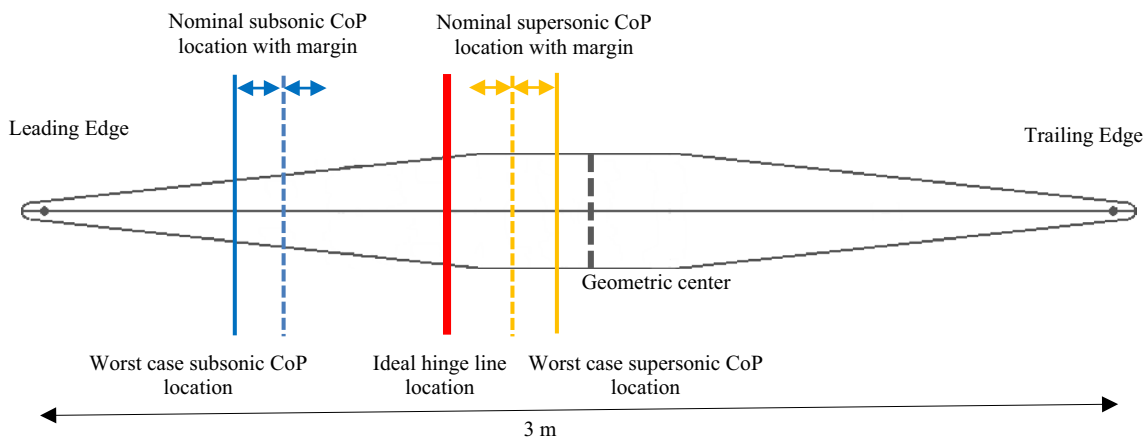


Fig. 5 Fin hinge line location

Table 2 Hinge moment estimations during control surface operation

	Aerodynamic contribution		Inertia contribution		Total moment	Required speed
Petal	890.3 kNm	3.4 kNm	893.7 kNm			2.5 rpm
Fin	128.4 kNm	0.5 kNm	128.9 kNm			1.7 rpm

during the unfolding phase, the drive into nominal position, and operations are very different. Unfolding and drive into nominal position require large rotations (90°), but the loads at these phases are relatively low on the fin, as these operations occur at high altitude, under low dynamic pressure. The operational actuators, while only need to rotate the fin by $\pm 20^\circ$ from the fin nominal position, are to work against very large aerodynamic loads. While the implementation of several actuators and locking increases mechanism complexity, it also allows for decoupling of load paths, therefore a single actuator is not required to satisfy the above presented contending requirements, and large aerodynamic loads do not flow through all mechanism components resulting in an overall more lightweight design. Furthermore, unfolding and operational mechanisms can be relatively independently tuned, facilitating easier testing and maintenance.

The main mechanism components are discussed below and are shown in Fig. 8.

The fork assembly interfaces with the fin structure through lugs with large-diameter bolts. The fork that is connected to a hollow tube houses a small linear actuator that unfolds the fin. The tube, in turn, is connected to the main axis. When the unfolding is complete, spring-activated pins slot into the pinholes of the fork and lugs to lock the axis, thus obtaining the fully deployed configuration shown on Fig. 6b.

The belt assembly is located around the main axis, shown on Fig. 9 in detail. Top and bottom belts are rigidly mounted to the main axis, which ends in the fork structure at one extremity. Both belts are equipped with two spring loaded pins, 180° apart. The central belt is mobile in-between the top and bottom belts. Following fin unfolding and the locking of axis 1, a small rotary actuator drives the fin into the nominal position through a small pinion and ring gear integrated into the top belt. When the induced 90° rotation is completed, the pins of the top and bottom belts slot in into the grooves of the central belt, thus locking axis 2, resulting in the nominal fin configuration depicted in Fig. 6c. All axis locking pins are resettable on ground.

Fin operation is driven by two large linear actuators. The axes being locked, the whole assembly of the main axis rotates when the operational actuators are engaged. A pair of large bearings on the main axis are sized to take radial loads, induced by the aerodynamic loading on the fins, as shown in Fig. 10. The large linear actuators are placed in a push–push configuration to create pure torque and avoid inducing undesired moments on the main axis.

The state of the art for large aerospace actuators (aircraft flight controls, landing gear, launch vehicles) are hydraulic actuators (HA), electro-hydrostatic actuators (EHA) and electromechanical actuators (EMA), the trend being towards using EMA both in the space and aircraft industry, replacing the more traditional hydraulic systems [4]. A trade-off of

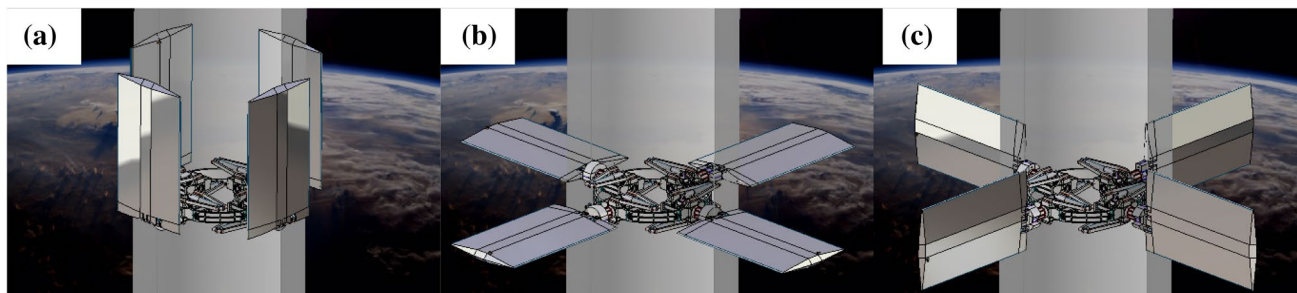


Fig. 6 Fin mechanism deployment sequence: **a** folded configuration; **b** fully deployed configuration with axis 1 locked; **c** nominal configuration with axis 2 locked

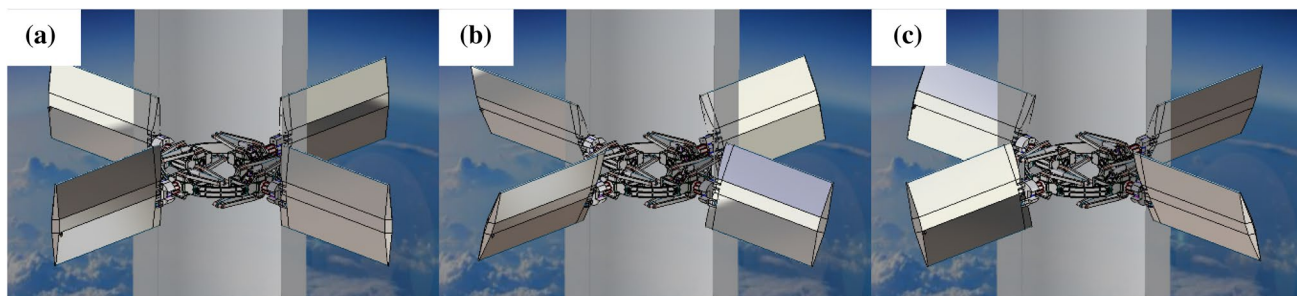
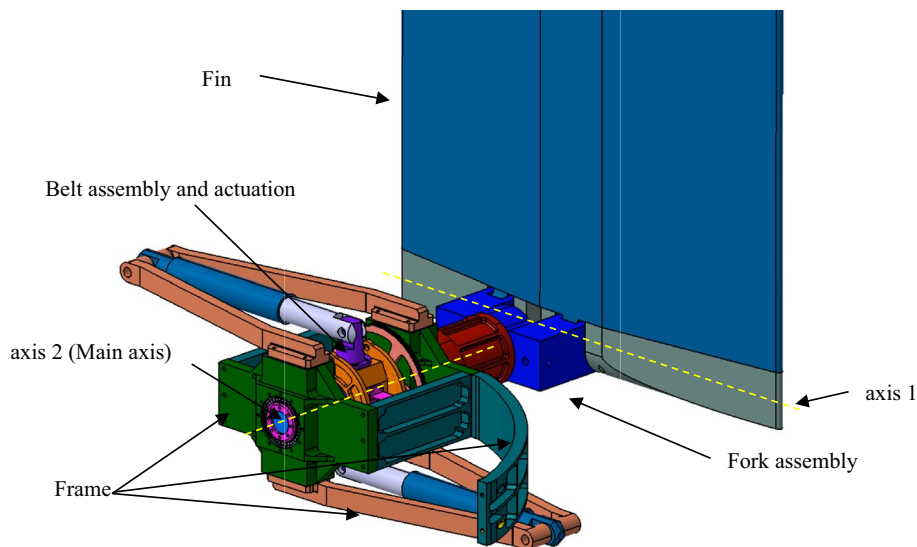


Fig. 7 Fin mechanism operation: **a** nominal deployed configuration; **b** $+20^\circ$ fin rotation; **c** -20° fin rotation

Fig. 8 Overview of fin actuation mechanism



these actuators was carried out, and candidates identified for fin operation are EMA and EHA used in launcher thrust vectoring applications, such as P120 from SABCA, used on the VEGA launch vehicle [5], and EHA offerings from Moog.

The main frame components are: bearing support, operational actuator support, longeron and cross-beam connecting the four fin mechanisms. To keep the mechanism mass as low as possible, wherever possible frame

components are foreseen to be made of carbon fiber reinforced polymer (CFRP), while machined components are foreseen to be made of aluminum wherever thermal or mechanical loads do not require the use of titanium components.

Fin locking is envisioned using shape memory alloy (SMA) actuators, such as Frangibolts: upon receiving the command, the SMA cylinder elongates to fracture

Fig. 9 Belt assembly, actuators and large bearings—full view and cut view

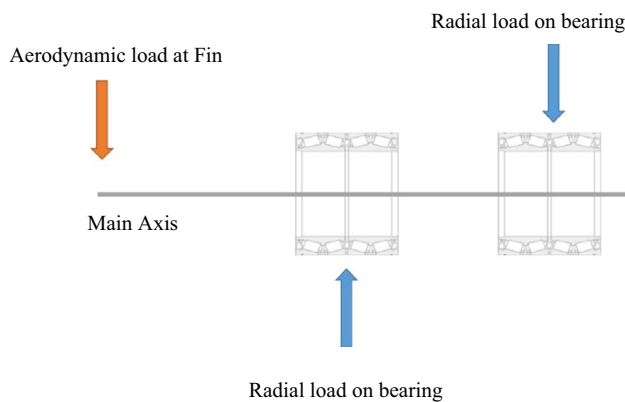
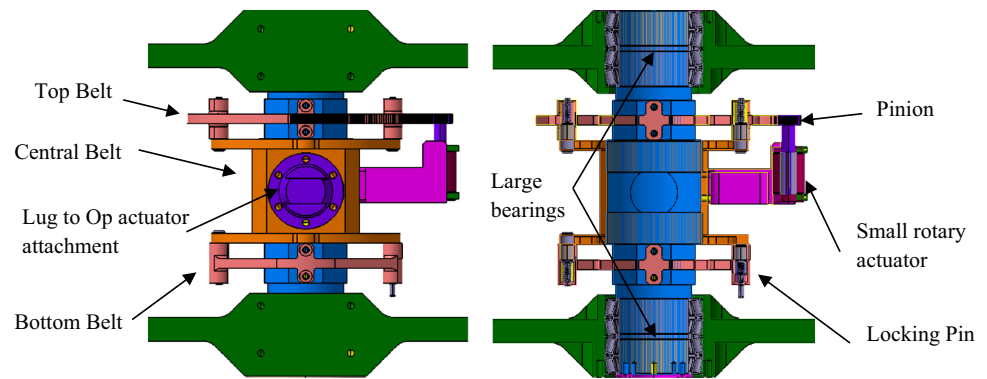


Fig. 10 Aerodynamic loading and induced radial loading on bearings

the bolt, and thus achieves separation. Such configuration also avoids the use of protruding elements.

4.1.6 Fin mechanism demonstrator

A fin-mechanism demonstrator is built to validate critical mechanism roles: to test the actuation chain and locking of axes through functional testing. The mechanism demonstrator is adjusted for a 1/5th scale, 1 m span, fin. The fin itself is supplied by MT Aerospace.

Actuation and locking functions, as well as component roles, are identical to those of the full-scale mechanism. The fin interface and axis 1 actuation are slightly modified for the demonstrator, to fit with the overall scaled geometry, as pure geometrical scaling results in a very small level arm for this actuator, and very high forces at the interface. All machined components are aluminum. Actuation is demonstrated with the help of hand wheels, and a single large actuator demonstrator is implemented rather than the dual actuation configuration of the full-scale model (Fig. 11).

4.2 Thrust vector control

4.2.1 Vectoring concept selection

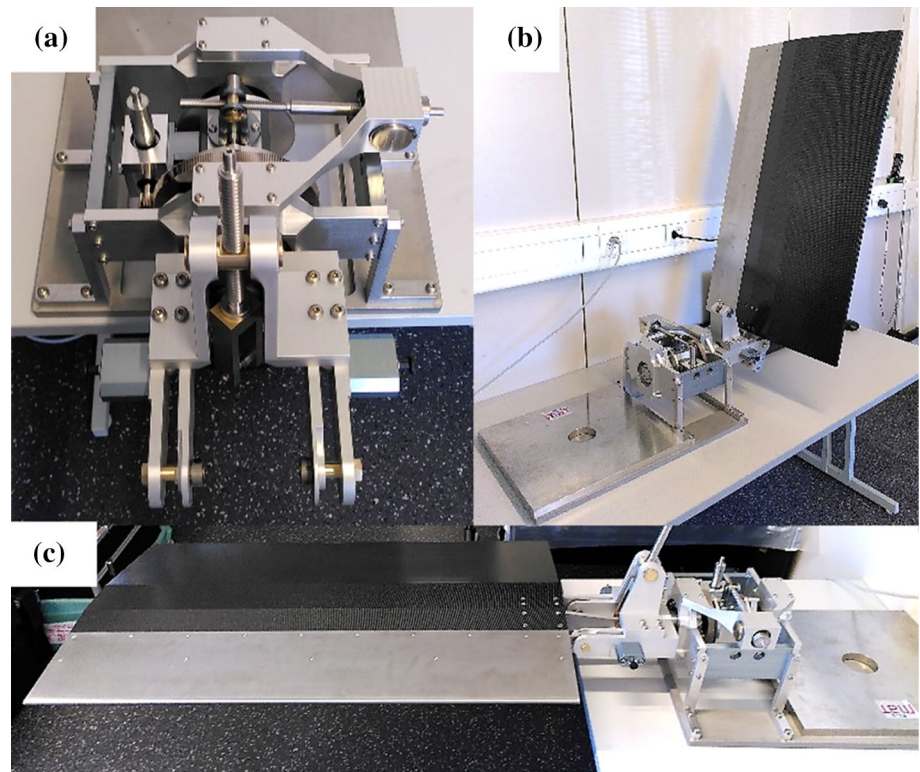
TVC mechanism design is considered for the requirements provided for the central engine during descent, as summarized in Table 3.

In general, vectoring approaches can be divided into vectoring using mechanical and fluidic systems. Fluidic vectoring systems use a fixed engine/nozzle assembly. Control is achieved through a secondary flow, interfering with the exhaust flow-stream. These systems are based on injection of fluid into the side of the diverging nozzle section, or at the exit of the nozzle, causing an asymmetrical distortion of the exhaust flow. The mechanical approach is usually based on mechanical deflection of the nozzle or of the thrust chamber, or insertion of heat-resistant movable bodies into the exhaust jet that experience aerodynamic forces and cause a deflection of part of the exhaust gas flow [6]. While mechanical flow deflection concepts may result in more compact solutions, ablative materials may need to be used on control surfaces. Secondary injection and mechanical deflection concepts require iteration loops with computational fluid dynamics (CFD) from early in the design; thus, the design and testing of such systems can be complex and costly. In contrast, concepts moving the engine/nozzle/array can be tested with dummies. These are the methods most commonly used on launchers and spacecraft.

It is assumed that the engine is delivered as a single component, and it is to be vectored as a whole, therefore the most suitable vectoring method has been identified as engine gimbaling, with the following main advantages: heritage, relatively low complexity, possibility of testing with dummy engine, no ablative surfaces needed, scalability, reliability, and relative ease of implementation of thermal decoupling. While disadvantages are the need for flexible piping, and potentially higher system mass with respect to some other vectoring methods.

Engine gimbaling can be achieved using a gimbal ring approach or a universal hinge approach. A gimbal ring

Fig. 11 Fin mechanism demonstrator: **a** mechanism, **b** fin-mechanism assembly in stowed configuration, **c** fin-mechanism assembly in deployed configuration



assembly can be placed around the thrust chamber: the engine is mounted within this annular interface ring. This ring is actuated and is connected to the middle stage mobile ring by two pivots 180° apart. The middle stage ring is connected to another interface ring at the base structure side through another set of pivots. Alternatively, the thrust chamber assembly can be suspended on a gimbal bearing/universal hinge. The hinge is connected to struts making up the thrust frame, providing the load path to the launcher base structure. The engine is deflected with the help of two linear actuators, attached to the thrust frame or launcher base structure on one side and to the engine on their piston side.

To apply the gimbal ring design on the RETALT1 engine, actuator interface rings of different diameters need to be used—with larger diameter at the launcher base structure interface side. Ring sizes are also a function of the engine interface geometry and available volume around the thrust chamber. Due to heritage and encumbrance the gimbal bearing option was chosen as baseline for RETALT1.

4.2.2 Baseline design overview

The gimbal bearing is a universal joint on which the engine is suspended; thus, it carries the thrust load. It is bolted to the engine above the thrust chamber, and at its upper flange it interfaces the thrust frame. Bearings at the actuator mounts are spherical plain bearings connecting to the engine on the piston side of the actuator, and to

the thrust frame or launcher base structure on the actuator rear side. Linear EMAs are chosen as baseline, with a lead screw converting the rotational motion of the motor to linear motion. Nominally, two actuators are spaced 90° degrees apart. Ideally, a direct drive configuration is considered, without gearbox, to reduce complexity and augment reliability. The main structural components of the TVC are the mounting brackets of the actuator and the engine thrust frame that transfers the thrust loads from the engine to the launcher base (Fig. 12).

Engine nozzle and thrust chamber contours have been defined by the project and they were expanded to an engine geometry, based on Vulcain 2 geometrical proportions [7]. Engine design and layout of engine components near the thrust chamber limit the placement of actuators, gimbal and thrust frame. It is expected that the engine is equipped with reinforced interface locations to be able to mount the vectoring actuator at either near the top or the bottom of the thrust chamber. Ideally, the moment arm between the actuators and gimbal axis should be maximized. Therefore, the actuator mount location is preferred at the lower interface ring below the engine throat. However, actuator mount locations, thus actuation components, should be protected by the launcher base thermal protection system (TPS), which, for RETALT1, is foreseen to be located above the engine throat, near the center of the thrust chamber. Therefore, nominally, engine mounts are located above the thrust

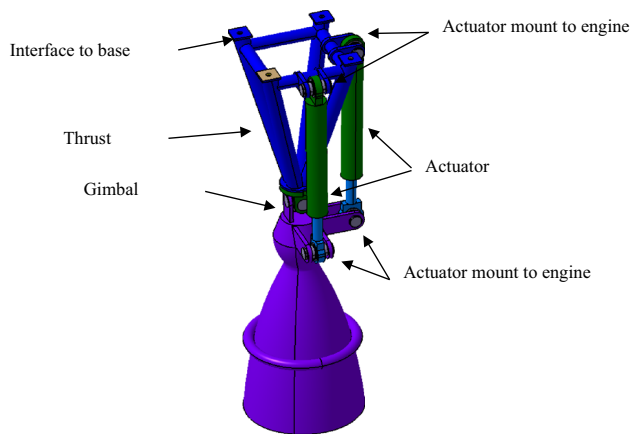


Fig. 12 RETALT1 engine outline, thrust frame and TVC layout

Table 3 Vectoring requirements

Requirement	Value
Axes	Pitch and yaw
Deflection angle/axis	$\geq \pm 6^\circ$
Deflection rate/axis	$\geq 10^\circ/\text{s}$
Supported mass	1700 kg
Nominal engine thrust level	1273 kN

chamber. Furthermore, an octaweb-like base structure, similar to that of Falcon 9, has been established below the main stage tank, to which the engines and TVC actuators are attached.

Main uses of power in launch vehicles are that of avionics, TVC, safeguard and pyro functions [9]. TVC actuators have high power demand. As baseline, EMA are considered for vectoring. While they can be lighter and more efficient than traditional hydraulic actuators, they also require more energy and power to operate. Therefore, energy storage options have been explored for thrust vectoring. Li-ion batteries have become the most popular power systems for space applications. These batteries, however, are slow to charge and discharge, and their power availability is limited. Thermal batteries (used for the VEGA TVC actuators [5]) are suitable for long duration storage—their electrolyte is inert at normal storage temperatures. These batteries need to be activated by an electrical or mechanical stimulus. Alternative to batteries are supercapacitors. While they are widely used in ground transport applications, currently they have no space heritage in Europe. However, they hold a great potential, due to their ability to charge and discharge instantly, their very high-power density, and their resilience to millions of life cycles [10].

4.2.3 Parametric model

Due to the absence of detailed TVC requirements, a generic vectoring concept was established, along with a parametric kinematic and torque model to be able to explore the design space and evaluate actuation needs and actuator specifications. Input parameters to this model include: vectoring performance, engine mass properties and geometry, and hinge/actuation mount locations.

The model consists of a planar kinematic model and an actuation torque model (Fig. 13). The kinematic model aids the evaluation of the actuator stroke required to move the engine to a given deflection angle. Actuation torque requirements are defined with respect to the gimbal point. The main torque contributions are: inertial torque, torques induced by engine thrust offset and misalignment, friction, piping and TPS stiffness, and disturbance torque due to vehicle linear and lateral accelerations [8]. For the preliminary torque estimation only inertial, thrust offset and misalignment torques are considered.

A baseline TVC configuration has been established with the assumptions presented in Table 4 and Fig. 14. The torque required to move the engine with these assumptions is 21 kNm. From kinematics, the required stroke for $\pm 6^\circ$ deflection is ± 52 mm. The actuator force is a function of the total torque required to move the engine and the lever arm from the gimbal pivot to the actuator mounting point. The derived actuator force requirement is 42.9 kN, and the linear speed requirement is 101 mm/s. The corresponding mechanical power output is on the order of 5 kW.

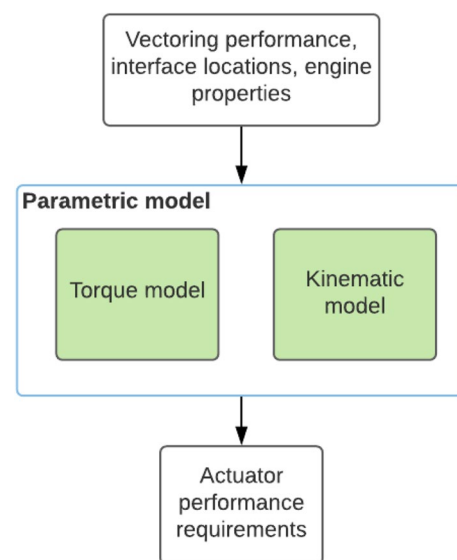
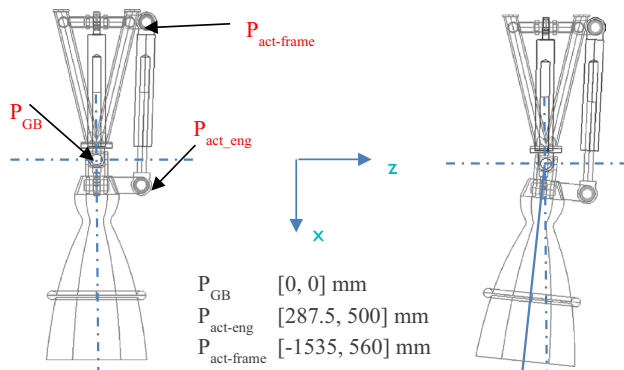


Fig. 13 TVC parametric model flowchart

Table 4 Assumptions for TVC parametric model

Parameter	Value
Engine inertia (at CoG)	[184, 465, 465] kg m ²
Angular misalignment	0.1°
Thrust offset	5 mm
Actuator inertia	0.03 kg m ²
Leadscrew lead	10 mm

**Fig. 14** TVC actuation kinematics—interface locations

Sensitivity analyses have been performed on the baseline configuration and a set of general design guidelines have been derived for the detailed design of the TVC mechanism:

- Gimbaled mass, center of gravity location as well as gimbaled inertia has a significant impact on required actuation needs. To reduce actuation needs, the pivot point shall be placed as close as possible to the engine CoG location.
- Actuator piston side attachment, near the vicinity of the engine CoG, can result in lower actuator force needs, as well as increasing the distance between the gimbal pivot and actuator mount location.
- Attachment of the actuators to the thrust frame and/or base structure impacts actuation kinematics and in turn thus actuator needs. In other words, actuation force and stroke needs can be tuned by kinematics through the actuator placement.
- Offset and misalignment are to be minimized. For the introduced preliminary sizing, 0.5 mm increase in misalignment results in nearly 5% increase for the actuator force.
- While it assumed that actuation components are protected from the landing-induced thermal environment by the base structure TPS, the TVC mechanism is impacted by the thermal environment induced by the propulsion subsystem. Some bearings are in the vicinity of the hot thrust chamber, while the thrust frame and actuator rear

mounts may be near the cryogenic tank, placing stringent thermal load requirements on the TVC. Some components might experience high thermal gradients, therefore the use of low thermal expansion and high strength materials, such as titanium, may be necessary. Furthermore, under cryogenic temperature conditions, liquid lubricants are not possible to use.

- The mechanical environment and stiffness requirements will drive structural sizing of the TVC and in turn, TVC structural mass.
- Furthermore, the number of engines to be vectored is a trade-off between mission/GNC needs, reliability and system (mass and power impact) considerations. The number of engines to be vectored and vectoring duty cycle will greatly impact the launcher power/energy budgets.

4.3 Landing legs

4.3.1 Landing leg concept selection

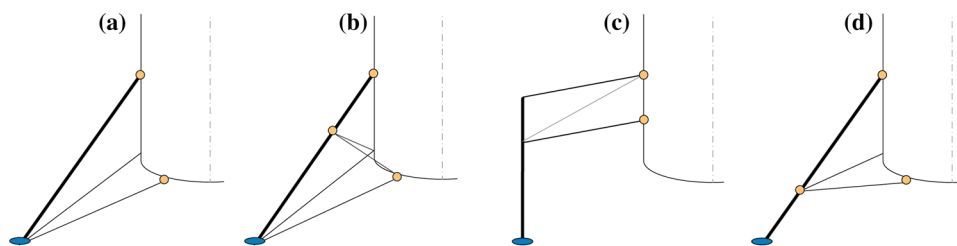
The main functional requirements of the landing legs are:

- The legs shall deploy fully and correctly and lock down in deployed position.
- The legs shall provide static and dynamic stability of the launcher, withstanding loads and conditions imposed by the environment.
- The landing legs shall protect the launcher against landing shocks. The legs need to cope with a residual landing speed and dissipate the impact energy at touch-down. This function is handled by the shock absorbing system. Due to the reusable nature of the launch vehicle, the method should allow for resetting or relatively easily replacement of the energy absorbing mechanism.
- The landing legs shall help maintaining adequate ground clearance between engine nozzle exit plane and the ground.

Three candidate architectures were identified for the landing legs: inverted tripod, parallel linkage, and cantilever configuration. A high-level description of each of these architectures is provided below and corresponding schematics are shown in Fig. 15.

For an inverted tripod configuration, the landing leg assembly consist of a primary strut and two secondary struts, all connected to the launcher with hinges. When deployed, the struts form an inverted tripod, with a joint at the foot of the landing legs. [11] At landing, forces are distributed along the strut axes. Such configuration is used on Falcon 9, and Blue Origin's New Glenn. Deployment of the legs can be achieved several ways, following the release of the hold-down latch: by telescopic actuation of the primary strut, or

Fig. 15 Leg architecture alternatives: **a** inverted tripod configuration requiring telescopic deployment; **b** inverted tripod configuration with locking struts; **c** parallel linkage mechanism; **d** cantilever mechanism



by segmentation of the primary strut, effectively unfolding the leg.

An alternative architecture is the parallel linkage concept: both the primary and secondary struts are folded against the vehicle body and locked with a hold-down and release mechanism (HDRM). They are deployed with the help of a linear actuator downward and outward, similar to the method used on Blue Origin's New Shepard. Movement of the legs can be approximated as a planar parallel linkage mechanism with the primary leg moving parallel to the vehicle body, a distance apart during deployment. Due to the vertical configuration of the primary strut, long secondary struts are needed to obtain a large enough stability footprint. As the secondary struts are attached to the primary strut at a larger distance from the footpad, bending of the primary strut is a risk.

The cantilever configuration is similar to that of the tripod one, however, the main strut meets the secondary struts further away from the foot. Such configuration requires relatively short secondary strut lengths; thus, they can be sized less massive to withstand buckling. The main strut is subject to bending, however, which poses a jamming risk of the mechanism. This configuration is commonly found on lunar and planetary landers. Deployment of the system can be achieved several ways; however, most methods require at least two actuators for the leg deployment.

Preliminary screening of the architectures was aided by simplified analysis of the leg configurations, considering a two-dimensional, vertical landing onto a uniform, flat surface. Required leg lengths were determined by assessing static stability of the launcher after landing. A preliminary mass estimation for each configuration was established based on the frame structure of CFRP struts. Static loads at landing were estimated, and strut cross sections chosen such as to obtain a positive margin of safety for the loading and buckling. Such preliminary sizing of the struts then allowed for estimating the mass of the strut structure.

Based on the preliminary assessment, the inverted tripod configuration was deemed to be most promising, in addition to its heritage of large reusable launcher (Falcon 9, New Glenn).

Reliability of deployment has been examined for telescopic and articulated configurations. Assuming that the landing system has to possess an overall reliability of 99%

per life cycle for the 4 legs, then presuming iso-probability of failure per leg, each landing leg shall have a reliability of 99.75% per life cycle. Such reliability requires the use of highly reliable architecture and components.

An architecture based on a telescopic boom similar to SpaceX concept was compared to an articulated strut architecture. The telescopic boom concept is appealing for its apparent simplicity but requires that the telescopic extension and locking are extremely reliable. To reach a 99.75% reliability of the whole leg mechanism, each latching system shall have a reliability of 99.937%, assuming 4 latching systems. Falcon 9 Jason-3 landing on the 17.01.2016 showed that locking failure may have catastrophic consequences, with tipping of the launcher after a successful approach, leading to explosion and total loss of the launcher [12].

The deployment kinematics of an articulated strut architecture is more complex but is based only on rotating parts around their respective axes which is the most reliable element in mechanisms. The reliability of the articulated struts architecture is located in the locking system instead of a multi-stage translational locking system of a telescopic boom. The reliability of the locking system is driven by the kinematics and dynamics of the landing leg deployment mechanism that are more predictable than tribology and complexity involved in a telescopic boom locking system. It is, thus, concluded that an articulated strut architecture presents a higher intrinsic reliability and lower development risks than a telescopic boom.

Leg deployment of an articulated structure can be actively actuated or passive. For active deployment, an EMA is placed within the launcher body, thus it is protected from thermal environment, and at impact it does not see landing loads. It deploys the legs through a small linkage mechanism. Actively (hydraulically) actuated folding legs are used in Blue Origin's New Glenn design [13]. For a passive configuration, upon releasing the HDRM, and using an initial kick spring, as the CoG is located away from the interface points to the launcher, the legs start deploying, driven by gravity. Such configuration can decrease mechanism complexity by avoiding the use of any actuator and control electronics, keeping cost and maintenance low (Fig. 16).

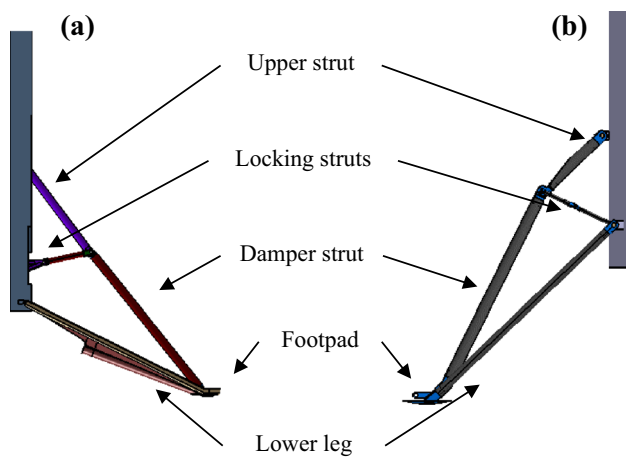


Fig. 16 Articulated landing leg configurations: **a** active—motorized, **b** passive—gravity-driven deployment

4.3.2 Baseline design overview

The lower legs interface the launcher at two interface points and support the footpad at their lower extremity. Near the footpad, a shaft provides interface to the damper strut. The damper strut houses the damping features. At full compression of the damping system, the damper strut and the upper strut align, so only tension is transmitted in the locking struts. The upper strut interfaces the damper strut and the upper launcher interface point.

The locking struts secure the landing leg structure once deployed. They connect the upper and damper struts to two lower launcher interfaces. Each strut is articulated to allow unfolding and folding. In addition, the locking strut hinge has a built-in end stop that limits the range of motion when deployed from its stowed position. The locking struts are maintained in extended position due to locking springs pulling the lower locking strut toward the deployed lower leg structure, applying a locking load on the hinge's mechanical end stop. This positive locking force is necessary to ensure locking once deployed and resist to potential parasitic forced due to vibration or inertial loads during final approach sequence.

At baseline, the attenuation mechanism is integrated into the bottom section of the damper strut: it is composed of a pneumatic/hydraulic damper and a crushable cartridge. The damper is connected to the main body of the damper strut on one side, and to the cartridge on the piston side. Cartridge and piston effectively move together with respect to the main cylinder of the damper strut. The damper absorbs the landing energy and is fully reusable under nominal landing. The crush cartridge does not crush during the nominal landing case, but aids load limitation under off-nominal landing cases by enhancing the shock attenuation ability of the leg. Under nominal landing conditions, the leg assembly does not

require refurbishment. Off-nominal loading results in further compression of the damper strut as the crushing cartridge engages. For this landing case, some refurbishment of the leg assembly, replacement of the cartridge is needed.

4.3.3 Concept of operations

Landing legs are stowed against the launcher body and held down by the HDRM mechanism, that retains the stowed configuration until deployment, during the ascent and descent phases. Upon command issued, latches unlock and release the legs: the tip of each leg is pushed away from the launcher body. Then, the landing leg is driven into deployed position: the lower legs and the damper strut rotate outward and the locking mechanism pushes outwards the knee formed by the damper and upper struts. Alternatively, the damper strut folds out of its stowed position with the help of a linear actuator.

The impact energy is absorbed by the compression of the damper leg: nominally the compression is equal to the stroke of the shock absorber. During this stroking the damper strut length reduces and the strut slightly rotates outward, while the foot itself slightly slides radially outward.

4.3.4 Kinematic and dynamic models

The detailed landing leg design requires establishment of several kinematic and dynamics models to ensure that the stowed configuration has a low encumbrance, deployment is possible and positive locking is achieved, as well as that the landing is feasible, and suitable dampers and cartridges can be procured. Furthermore, such models are essential to structurally size the legs.

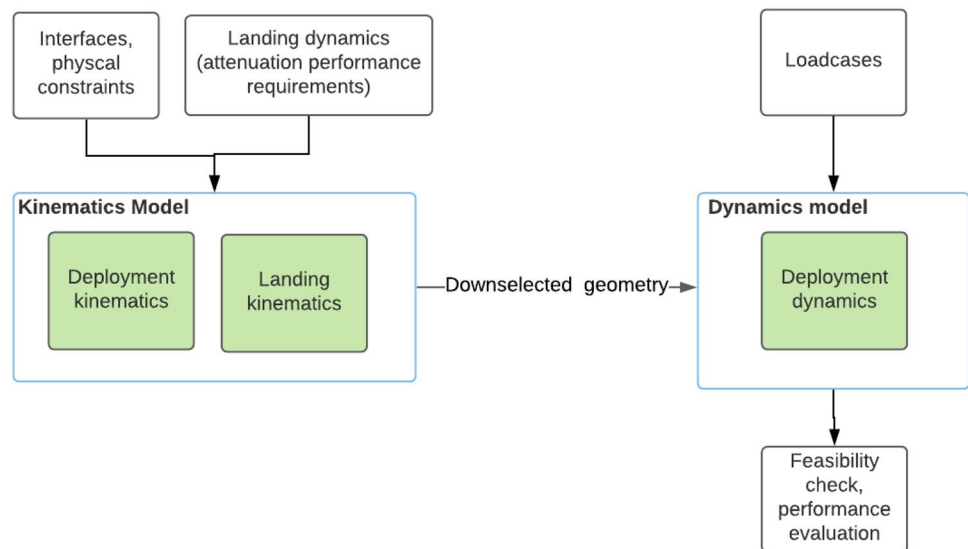
Landing dynamics is modeled by MT Aerospace, and outputs regarding the required damping performance are provided to Almatech.

Almatech has established an integrated model (Fig. 17) consisting of kinematic models for both deployment and landing to be able to optimize the length of the upper and damping struts to ensure reliable deployment while minimizing encumbrance of the stowed configuration. The landing kinematics model aids derivation of requirements for the damping subsystem. Additionally, a deployment dynamics model is established to aid the verification and deployment of the locking sequence.

4.3.5 Landing leg mechanism demonstrators

A deployment mechanism demonstrator is foreseen to be built to validate the deployment concept under 1 g loading. Functional testing will demonstrate the deployment mechanism main functions: unlocking, deployment kinematics and strut locking.

Fig. 17 Landing leg models flowchart



Additionally, a scaled landing test is planned, where a single leg is fitted into a drop tower to validate the structural performance of the leg and the dynamic performance of the shock attenuation.

5 Conclusions and outlook

This paper gives an overview of Almatech activities in the RETALT project on mechanism concepts for the aerodynamic control surfaces, thrust vector control and landing legs for the RETALT1 launch vehicle. The activities for the aerodynamic control surfaces have been completed, including construction of a reduced scaled demonstrator. The thrust vector control preliminary design is also finalized and is presented in detail including concept trade-off. Finally, the landing leg preliminary concept design trade-off is finalized; however, the preliminary design could not be presented due to ongoing activities.

Acknowledgements The RETALT project has received funding from the European Union's Horizon 2020 research and innovation framework program under Grant agreement No. 821890.

Open Access This article is licensed under a Creative Commons Attribution 4.0 International License, which permits use, sharing, adaptation, distribution and reproduction in any medium or format, as long as you give appropriate credit to the original author(s) and the source, provide a link to the Creative Commons licence, and indicate if changes were made. The images or other third party material in this article are included in the article's Creative Commons licence, unless indicated otherwise in a credit line to the material. If material is not included in the article's Creative Commons licence and your intended use is not permitted by statutory regulation or exceeds the permitted use, you will need to obtain permission directly from the copyright holder. To view a copy of this licence, visit <http://creativecommons.org/licenses/by/4.0/>.

References

1. Marwege, A., Gülhan, A., Klevanski, J., Riehmer, J., Kirchheck, D., Karl, S., Bonetti, D., Vos, J., Jevons, M., Krammer, A., Carvalho, J.: Retro propulsion assisted landing technologies (RETALT): current status and outlook of the EU funded project on reusable launch vehicles. In: 70th International Astronautical Congress (IAC), Washington D.C., USA (2019)
2. De Zaiacomo, G., Blanco Arnao, G., Bunt, R., Bonetti, D.: Mission engineering for the RETALT VTVL launcher, CEAS (2021) (**under review**)
3. Charbonnier, D., Vos, J., Marwege, A., Hantz, C.: Computational fluid dynamics investigations of aerodynamic control surfaces of a vertical landing configurations, CEAS (2021) (**under review**)
4. Qiao, G., Liu, G., Shi, Z., Wang, Y., Ma, S., Lim, T.: A review of electromechanical actuators for more/all electric aircraft systems. *J. Mech. Eng. Sci.* **232**(22), 4128–4151 (2018)
5. Carnevale, C., Resta, P.: Vega electromechanical thrust vector control development. <https://doi.org/10.2514/6.2007-5812> (2007)
6. Sutton, G.P., Biblarz, O.: *Rocket Propulsion Elements*. Wiley, New York (2001)
7. Schneider, D., Génin, C., Stark, R., Fromm, C.: Ariane 5 performance optimization using dual bell nozzle extension. In: Proceedings of the 4th Space Propulsion Conference, Köln, Germany (2014)
8. Ganesh, B., Jhanwar, R., Kodeeswaran, M., Prakash, B., Kumar, P.R.: Design of 25 kW redundant linear electro-mechanical actuator for thrust vector control applications. In: Proceedings of the 1st International and 16th National Conference on Machines and Mechanisms (iNaCoMM2013), pp 1033–1039 (2013)
9. Van Renterghem, D., Bekemans, M., Brochard, P., Simon, E.: Sources for high power/energy demanding applications inside-launchers. In: Proceedings of the 10th European Space Power Conference, Noordwijkerhout, Netherlands. vol. 719. ESA Special Publication (2014)
10. New supercapacitor cell for launchers: https://www.esa.int/Enabling_Support/Space_Engineering_Technology/Shaping_the_Future/New_supercapacitor_cell_for_launchers (2020). Accessed 30 June 2021
11. Witte, L.: Touchdown dynamics and the probability of terrain related failure of planetary landing systems—a contribution to

- the landing safety assessment process. <https://doi.org/10.13140/RG.2.1.4334.4405>. (2015).
12. Foust, J.: Falcon 9 launches Jason-3 satellite but landing attempt fails: <https://spacenews.com/falcon-9-launches-jason-3-satellite-landing-attempt-fails/> (2016). Accessed 30 June 2021
 13. Landing Gear: <https://www.blueorigin.com/new-glenn/> (2021). Accessed 30 June 2021

Publisher's Note Springer Nature remains neutral with regard to jurisdictional claims in published maps and institutional affiliations.